Journal of Organometallic Chemistry 882 (2019) 50–57

Contents lists available at ScienceDirect

Journal of Organometallic Chemistry

journal homepage: www.elsevier.com/locate/jorganchem

Reactions of POCOP pincer palladium benzylthiolate complexes with $BH_3 \cdot THF$: Isolation and characterization of unstable POCOP-Pd(η^1-HBH_3) complexes

Jie Zhang[*], Yazhou Ding, Qiang-Qiang Ma, Bula Cao, Jiarui Chang, Shujun Li, Xuenian Chen[**]

School of Chemistry and Chemical Engineering, Henan Key Laboratory of Boron Chemistry and Advanced Energy Materials, Henan Normal University, Xinxiang, Henan, 453007, China

A R T I C L E I N F O

Article history:
Received 12 November 2018
Received in revised form
20 December 2018
Accepted 31 December 2018
Available online 3 January 2019

Keywords:
Palladium
Borane
Tetrahydroborate complex
Pincer complex
Coordination mode

A B S T R A C T

In order to explore the boron mediated C-S bond activation of the thiolate ligand in transition metal thiolate complexes, several bis(phosphinite) (POCOP) pincer ligated palladium complexes bearing a benzylthiolate or mercapto auxiliary ligand, $[2,6\text{-}(R_2PO)_2C_6H_3]PdY$ ($Y = SCH_2Ph$, $R = {}^tBu$, **1a**, ${}^iPr$, **1b**; $Y = SH$, $R = {}^tBu$, **2a**, ${}^iPr$, **2b**), were synthesized and fully characterized by multinuclear NMR, FTIR, X-ray crystallography and elemental analysis. The reactions of complexes **1a-b** or **2a-b** with $BH_3 \cdot THF$ at room temperature produced exclusively the corresponding tetrahydroborate complexes, $[2,6\text{-}(R_2PO)_2C_6H_3]Pd(\eta^1\text{-}HBH_3)$ ($R = {}^tBu$, **3a**; ${}^iPr$, **3b**), through Pd-S bond cleavage. Complexes **3a** and **3b** are air/moisture sensitive and thermally unstable. X-ray crystallography and FTIR spectra supported a η^1-HBH_3 monodentate coordination mode for the BH_4 ligand in complexes **3a** and **3b**. The boron mediated C-S bond cleavage was not observed in the reactions of complexes **1a** and **1b** with $BH_3 \cdot THF$ perhaps due to the relatively weak Pd-S bond.

1. Introduction

The activation of C—S bond has received substantial attentions in recent years due to the fact that C—S bond exists extensively in the molecules of natural products, drugs and pesticides [1–7]. Up to now, most researches on the C—S bond activation are focused on thioesters and thioethers and the activations are usually achieved via transition metal mediated or catalyzed processes. Comparatively, very few reports are available for the C—S bond activation of thiophenols and mercaptans [1]. Recently, we found that BH_3 species can mediate the C—S bond cleavage of the benzylthiolate auxiliary ligand in bis(phosphinite) (POCOP) pincer ligated nickel complexes [8]. The treatment of $[2,6\text{-}({}^tBu_2PO)_2C_6H_3]NiSCH_2Ph$ with 2 equiv of $BH_3 \cdot THF$ in benzene at room temperature led to the formation of $[2,6\text{-}({}^tBu_2PO)_2C_6H_3]NiSH$. It was believed that this nickel mercapto complex was formed through BH_3 induced C-S bond cleavage: the coordination of S to B followed by a hydride transfer from B to S and the benzyl group transfer from S to B (Chart 1) resulted in the formation of the nickel mercapto complex. In order to further explore this reactivity, we extended the chemistry to the corresponding palladium complexes. In this paper, we synthesized POCOP pincer palladium complexes $[2,6\text{-}(R_2PO)_2C_6H_3]PdSCH_2Ph$ ($R = {}^tBu$, **1a**; ${}^iPr$, **1b**) and reacted them with $BH_3 \cdot THF$ under the same conditions. However, the expected C—S bond cleavage of the benzylthiolate auxiliary ligand in **1a** and **1b** was not observed perhaps due to the relatively weak Pd-S bond. Nevertheless, two air/moisture sensitive thermally unstable POCOP pincer palladium tetrahydroborate complexes, $[2,6\text{-}(R_2PO)_2C_6H_3]Pd(\eta^1\text{-}HBH_3)$ ($R = {}^tBu$, **3a**; ${}^iPr$, **3b**), were obtained and structurally characterized. To our knowledge, transition metal complexes with a η^1-HBH_3 monodentate tetrahydroborate ligand are very difficult to be isolated and the crystal structures of this type of complexes have rarely been reported [9,10].

2. Results and discussion

2.1. Syntheses, characterization and crystal structures of $[2,6\text{-}(R_2PO)_2C_6H_3]PdSCH_2Ph$ ($R = {}^tBu$, 1a; ${}^iPr$, 1b)

We previously reported the synthesis of complex **1b** through the reaction of $NaSCH_2Ph$ with $[2,6\text{-}({}^iPr_2PO)_2C_6H_3]PdCl$ in THF under a

---

[*] Corresponding author.

[**] Corresponding author.

E-mail addresses: jie.zhang@htu.edu.cn (J. Zhang), xnchen@htu.edu.cn (X. Chen).

https://doi.org/10.1016/j.jorganchem.2018.12.019

reflux condition [11]. Complex **1a** was synthesized similarly in this work (Scheme 1).

The pincer backbone survived this reaction although most POCOP pincer ligands are unstable under extreme basic conditions [12]. Complex **1a** is an air stable yellow crystalline solid. $^{31}P\{^1H\}$ NMR spectroscopy indicated that no significant decomposition occurred when a THF-d_8 solution of **1a** was exposed to air for a few days. However, **1a** is unstable in chloroform or dichloromethane solution. ^1H and $^{31}P\{^1H\}$ NMR spectra showed that **1a** was slowly converted back to the chloride complex in a $CDCl_3$ or CD_2Cl_2 solution even at room temperature. This reactivity is similar to that of *trans*-$[Pd(Et)(SPh)(PMe_3)_2]$, which reacts slowly with organic halides such as allyl chloride, benzyl bromide and methyl iodide to form the corresponding palladium halide complexes [13]. The same reactivity was also observed for complex **1b** [11].

Complex **1a** was characterized by NMR, X-ray crystallography and elemental analysis. The ^1H, $^{13}C\{^1H\}$ and $^{31}P\{^1H\}$ NMR spectra of **1a** (Appendix A, Fig. A1–A3) supported the structure shown in Scheme 1. The expected spectra features for a POCOP pincer palladium complex [11,14] were also displayed in the NMR spectra of **1a**. The $^{31}P\{^1H\}$ NMR spectrum showed one singlet, implying that the two $^tBu_2PO$ arms were equivalent in solutions.

Single crystal X-ray diffraction analyses for **1a** and **1b** were carried out at room temperature using a SuperNova diffractometer (Oxford Diffraction) to get information about the structures of these complexes. The molecular structures of **1a** and **1b** are shown in Figs. 1 and 2 with selected bond lengths and angles listed.

Similar to other reported POCOP pincer palladium complexes [11,14], the square-planar geometry for the palladium center is distorted in the molecules of **1a** and **1b**. This structure feature is also very common for the related pincer nickel complexes [8,12,15–30]. The C_{ipso}-Pd bond lengths in **1a** and **1b** (2.010(2) and 2.013(6) Å) are quite similar to those of the related POCOP pincer palladium complexes (2.000(4)–2.015(2) Å) [11]. No significant difference was observed for the Pd-S bond lengths of **1a** and **1b** (2.3679(7) and 2.3429(19) Å for **1a** and **1b**, respectively). The Pd-S bond lengths observed in this work are comparable to those of the corresponding pincer palladium complexes (2.3635(8)–2.3745(12) Å) [11] and that of *trans*-$[Pd(Et)(SPh)(PMe_3)_2]$ (2.384(2) Å) [31], however, they are much longer than those of other palladium(II) thiolate complexes with a square-planar geometry [32,33]. For example, in complex $[Pd(SR)_2(TMEDA)]$ (TMEDA = tetramethylethylenediamine; R = C_6F_5, C_6F_4-4-H, C_6H_4-2-$SiPh_3$), the Pd–S bond lengths are between 2.2696(9) and 2.2900(6) Å [32]. This indicates that the Pd–S bonds in the present POCOP pincer palladium complexes are relatively weak. The result is in good agreement with the experimental observation that these palladium thiolate complexes were slowly converted to chloride complexes in $CHCl_3$ or CH_2Cl_2 solutions. For the POCOP pincer nickel mercapto/thiolate complexes, the Ni-S bond length of a mercapto or an aliphatic thiolate complex is slightly shorter than that of the corresponding aromatic thiolate complex [21]. However, for the POCOP pincer palladium thiolate complexes, the Pd-S bond lengths are not significantly influenced by the substituents on the phosphine arms or the substituents on the sulfur atoms as indicated by the crystallography data of this work and the crystallography data of the POCOP pincer palladium aromatic thiolate complexes reported previously [11].

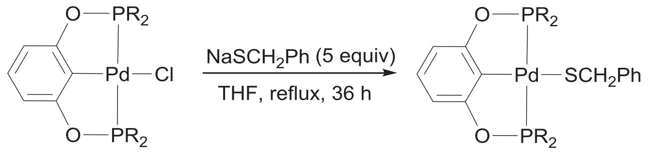

R = ^{t}Bu, **1a** (78%); ^{i}Pr, **1b**

Scheme 1. Syntheses of complexes **1a** and **1b**.

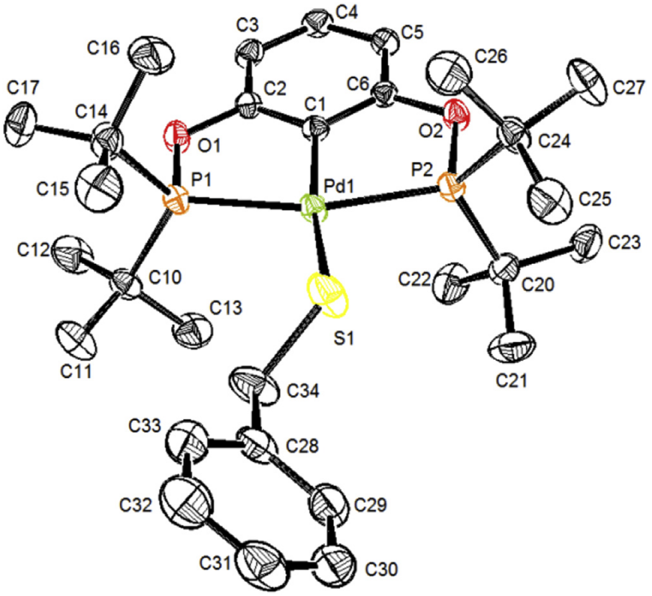

Fig. 1. Thermal ellipsoid plots of complex **1a** at the 50% probability level (hydrogen atoms are omitted for clarity). Selected bond lengths (Å) and angles (deg): Pd1-C1, 2.010(2); Pd1-P1, 2.3171(6); Pd1-P2, 2.2816(6); Pd1-S1, 2.3679(7); S1-C34, 1.801(3); P1-Pd1-P2, 159.04(2); S1-Pd1-C1, 170.14(7); P1-Pd1-S1, 107.24(3); P2-Pd1-S1, 93.70(2); Pd1-S1-C34, 112.21(11).

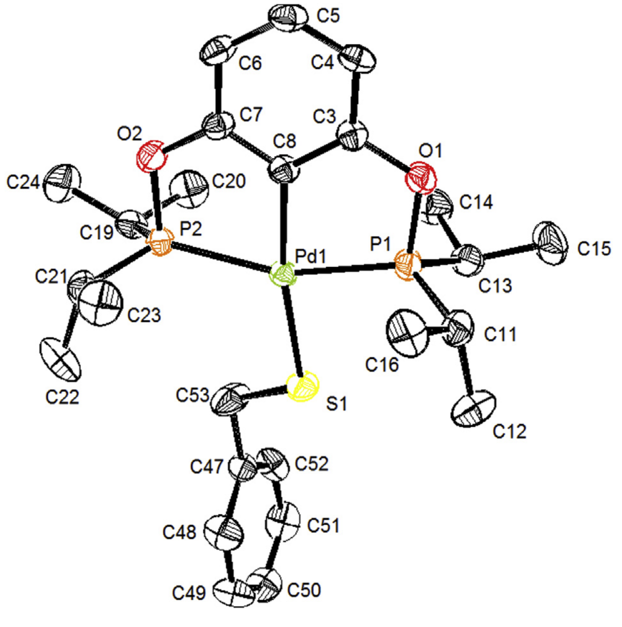

Fig. 2. Thermal ellipsoid plots of complex **1b** at the 50% probability level (two independent molecules were found in the crystalline lattice; only one is shown here; hydrogen atoms are omitted for clarity). Selected bond lengths (Å) and angles (deg): Pd1-C8, 2.013(6); Pd1-P1, 2.2495(19); Pd1-P2, 2.2892(19); Pd1-S1, 2.3429(19); S1-C53, 1.807(9); P1-Pd1-P2, 159.26(7); S1-Pd1-C8, 170.8(2); P1-Pd1-S1, 91.66(7); P2-Pd1-S1, 109.01(7); Pd1-S1-C53, 110.4(3).

*2.2. Syntheses, characterization and crystal structures of [2,6-($R_2PO)_2C_6H_3$]PdSH (R = ^{t}Bu, **2a**; ^{i}Pr, **2b**)*

The purpose of this work is to investigate the BH$_3$ mediated C-S bond cleavage of the benzylthiolate auxiliary ligand in complexes **1a** and **1b**. If this process occurred, the corresponding palladium mercapto complexes, [2,6-($R_2PO)_2C_6H_3$]PdSH (R = ^{t}Bu, **2a**; ^{i}Pr, **2b**), would be detected. In order to monitor the interactions of **1a** and **1b** with BH$_3$·THF more conveniently, complexes **2a** and **2b** were synthesized (Scheme 2) and fully characterized.

The methods used for the syntheses of **2a** and **2b** were similar to that used for the syntheses of the corresponding nickel mercapto complexes as described previously [8,21]. However, it should be noted that the present reactions were carried out in pure THF under a reflux condition and 2 equiv of NaSH was used. The yields could be significantly low or the expected products could not be isolated if a large amount of excess NaSH was employed. Similar to **1a** and **1b**, complexes **2a** and **2b** are light yellow to orange crystalline solids and are air stable in solid state. However, they are lightly air sensitive in solutions and were slowly converted back to the starting chloride complexes in chloroform or dichloromethane solutions at room temperature as complexes **1a** and **1b**.

The structures of **2a** and **2b** depicted in Scheme 2 were supported by NMR and FTIR spectra (Appendiix A, Fig. A4–A11). Like the corresponding pincer nickel mercapto complexes [8,21], the ^{1}H NMR resonances of the SH protons of **2a** and **2b** appeared in relatively high field (−0.74 ppm for **2a** and −1.03 ppm for **2b**) as virtual triplets. However, the H-P coupling constants (10–12 Hz) were smaller than those of the nickel mercapto complexes (17–20 Hz) [8,21]. Similar ^{1}H NMR resonances and H-P coupling constants were previously reported for other transition metal mercapto complexes [34–36]. The ^{31}P{^{1}H} NMR spectra of **2a** and **2b** showed one singlet as expected, indicating that the two phosphine arms were identical in solutions. The FTIR spectra of **2a** and **2b** showed weak absorptions at 2587 and 2567 cm^{-1}, respectively, corresponding to the S–H stretching vibration.

The structures of **2a** and **2b** were further confirmed by single crystal X-ray diffraction analyses using a SuperNova diffractometer (Oxford Diffraction). The molecular structures of **2a** and **2b** are shown in Figs. 3 and 4 and the selected bond lengths and angles are also provided.

With a distorted square-planar geometry for the palladium center, the molecular structures of **2a** and **2b** are analogous to those of **1a**, **1b** and other reported POCOP pincer palladium complexes [11,14].

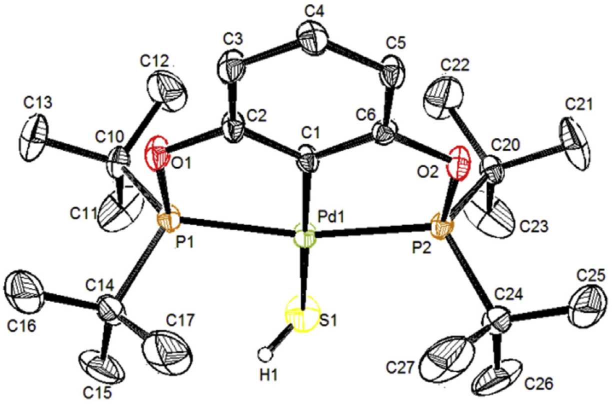

Fig. 3. Thermal ellipsoid plots of complex **2a** at the 50% probability level (hydrogen atoms except that attached to sulfur are omitted for clarity). Selected bond lengths (Å) and angles (deg): Pd1-C1, 2.011(4); Pd1-P1, 2.2934(13); Pd1-P2, 2.2923(13); Pd1-S1, 2.3691(15); P1-Pd1-P2, 159.25(5); S1-Pd1-C1, 178.83(15); P1-Pd1-S1, 100.93(6); P2-Pd1-S1, 99.78(5).

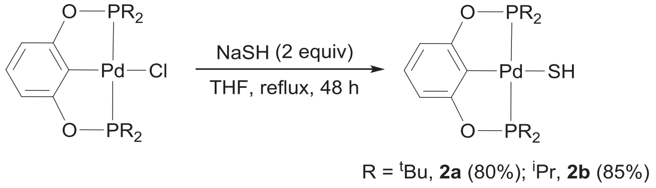

Scheme 2. Syntheses of complexes **2a** and **2b**.

*2.3. Reactions of **1a** and **1b** with BH$_3$·THF and isolation of [2,6-($R_2PO)_2C_6H_3$]Pd(η^1-HBH$_3$) (R = ^{t}Bu, **3a**; ^{i}Pr, **3b**)*

We previously reported that POCOP pincer nickel benzylthiolate complexes can react with BH$_3$·THF to form the corresponding nickel hydride complexes. Further reactions of the nickel hydride species with BH$_3$·THF can produce the corresponding tetrahydroborate complexes. Particularly, the reaction of [2,6-(^{t}Bu$_2$PO)$_2$C$_6$H$_3$]NiSCH$_2$Ph with 2 equiv of BH$_3$·THF in benzene at room temperature for 48 h can lead to the C-S bond cleavage of the benzylthiolate auxiliary ligand [8]. In order to explore this reactivity more extensively, we reacted **1a** and **1b**, respectively, with BH$_3$·THF under the same conditions.

Complex **1a** or **1b** (0.5 mmol) was mixed with BH$_3$·THF (1 mmol) in benzene-*d*$_6$ (5 mL) under a nitrogen atmosphere. The mixture was stirred at room temperature and the reaction was monitored by ^{31}P{^{1}H} and ^{11}B NMR spectroscopy. For both the reactions, the ^{31}P{^{1}H} NMR spectra showed that the original resonance due to the starting complex (**1a** or **1b**) disappeared completely in 1 h and an unknown resonance at 200.21 ppm (for the reaction of **1a** with BH$_3$·THF) or 195.43 ppm (for the reaction of **1b** with BH$_3$·THF) appeared. The ^{11}B NMR spectra showed a broad singlet at −13.50 ppm along with an unknown quintet at −39.82 ppm (for the reaction of **1a** with BH$_3$·THF) or −39.54 ppm (for the reaction of **1b** with BH$_3$·THF). The broad singlet at −13.50 ppm was in good agreement with a trimeric thioborane compound (PhCH$_2$SBH$_2$)$_3$ reported previously [8]. The reaction mixture was further stirred

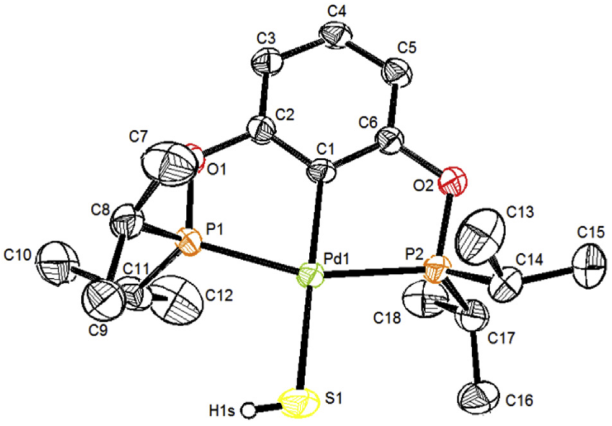

Fig. 4. Thermal ellipsoid plots of complex **2b** at the 50% probability level (hydrogen atoms except that attached to sulfur are omitted for clarity). Selected bond lengths (Å) and angles (deg): Pd1-C1, 2.013(3); Pd1-P1, 2.2641(7); Pd1-P2, 2.2698(7); Pd1-S1, 2.3529(9); P1-Pd1-P2, 159.58(3); S1-Pd1-C1, 179.59(8); P1-Pd1-S1, 100.50(3); P2-Pd1-S1, 99.80(3).

and monitored at room temperature for 72 h. However, no significant change was observed except that a trace amount of a previously reported hydride species [14] [2,6-(^{t}Bu$_2$PO)$_2$C$_6$H$_3$]PdH (for the reaction of **1a** with BH$_3$·THF) or [2,6-(^{i}Pr$_2$PO)$_2$C$_6$H$_3$]PdH (for the reaction of **1b** with BH$_3$·THF) developed at the later stage as indicated by the ^{31}P{^{1}H} NMR spectra. The expected C-S bond cleavage product, **2a** or **2b**, was not observed.

Preparative scale experiments for the reactions of **1a** and **1b** with BH$_3$·THF were carried out, respectively, in order to isolate the unknown species formed in the above reactions. Complex **1a** or **1b** (1 mmol), BH$_3$·THF (2 mmol), benzene (10 mL) were added to a flask under a nitrogen atmosphere. After the mixture was stirred at room temperature for 1 h, the solution was concentrated to 5 mL and kept under a nitrogen atmosphere at room temperature. Colorless crystals developed for both the mixtures after a few days. The crystals were separated and characterized by ^{1}H, ^{31}P{^{1}H}, ^{13}C{^{1}H} and ^{11}B NMR spectroscopy. For the crystals collected from the reaction mixture of **1a** with BH$_3$·THF, the NMR spectra were consistent with [2,6-(^{t}Bu$_2$PO)$_2$C$_6$H$_3$]Pd(η^1-HBH$_3$) (**3a**). For the crystals collected from the reaction mixture of **1b** with BH$_3$·THF, the NMR spectra were in good agreement with [2,6-(^{i}Pr$_2$PO)$_2$C$_6$H$_3$]Pd(η^1-HBH$_3$) (**3b**). The reactions of complexes **1a** and **1b** with BH$_3$·THF are summarized in Scheme 3. The NMR spectra of complexes **3a** and **3b** are provided in Appendix A (Fig. A12–A19).

2.4. Reactions of **2a** and **2b** with BH$_3$·THF

POCOP pincer nickel mercapto complexes are very reactive towards BH$_3$·THF to form the corresponding nickel tetrahydroborate complexes and THF·BH$_2$-μ_2-S(B$_2$H$_5$) [21]. It is likely that the palladium mercapto complexes **2a** and **2b** react similarly against BH$_3$·THF. To confirm that the C-S bond cleavage products **2a** and **2b** were not formed rather than were consumed by reacting with BH$_3$·THF, we checked the interactions of **2a** and **2b** with BH$_3$·THF, respectively. Complex **2a** or **2b** (0.1 mmol) was treated with 6 equiv of BH$_3$·THF in benzene-d_6 (0.5 mL) in a NMR tube under a nitrogen atmosphere and the reaction was monitored by ^{31}P{^{1}H} and ^{11}B NMR spectra. For both the reactions, the ^{11}B NMR spectra showed the formation of THF·BH$_2$-μ_2-S(B$_2$H$_5$) [21,37]. The ^{31}P{^{1}H} NMR spectra indicated that the starting complexes reacted completely in 30 min. Complex **3a** formed for the reaction of **2a** with BH$_3$·THF and complex **3b** formed for the reaction of **2b** with BH$_3$·THF as evidenced by both the ^{31}P{^{1}H} and ^{11}B NMR spectra. The reactions of complexes **2a** and **2b** with BH$_3$·THF are summarized in Scheme 4.

During the interaction of **1a** or **1b** with BH$_3$·THF, if the C-S bond cleavage product (**2a** or **2b**) formed and subsequently consumed by further reacting with BH$_3$·THF, the boron compound THF·BH$_2$-μ_2-S(B$_2$H$_5$) should be detected in the reaction system. However, the ^{11}B NMR spectra did not show the resonances due to THF·BH$_2$-μ_2-S(B$_2$H$_5$).

For the boron mediated C-S bond cleavage of the benzylthiolate ligand in POCOP pincer nickel benzylthiolate complex, the bond cleavage is believed to occur through the process as depicted in Chart 1 [8]. However, it is likely that the process depicted in Chart 2 take place exclusively in the cases of POCOP pincer palladium benzylthiolate complexes due to the relatively weak Pd-S bond. Because of this reason, the boron mediated C-S bond cleavage of the benzylthiolate ligand in the palladium benzylthiolate complexes was not observed.

2.5. Instability and molecular structures of complexes **3a** and **3b**

Both **3a** and **3b** are air/moisture sensitive thermally unstable colorless complexes. Attempts to obtain solvent-free dry samples of **3a** and **3b** for the purpose of elemental analysis were not successful. When the samples were dried under a dynamic vacuum or a nitrogen stream at room temperature, **3a** and **3b** were slowly converted to the corresponding palladium hydride species [14] by losing the BH$_3$ moiety as indicated by the ^{31}P{^{1}H} NMR spectra. The two phosphine atoms in complexes **3a** and **3b** were equivalent in solutions as the ^{31}P{^{1}H} NMR spectrum of **3a** or **3b** showed only one singlet.

Previously, we reported the structures and reactivities of the corresponding POCOP pincer nickel tetrahydroborate complexes [2,6-(R$_2$PO)$_2$C$_6$H$_3$]Ni(η^2-H$_2$BH$_2$) (R = ^{t}Bu, **4a**; ^{i}Pr, **4b**) [28]. The ^{1}H NMR resonances of the B*H*$_4$ moiety in complexes **4a** and **4b** appeared in relatively high field: −0.45 (benzene-d_6) and −1.13 (dichloromethane-d_2) ppm for **4a**; −0.71 (benzene-d_6) and −1.39 (dichloromethane-d_2) ppm for **4b**. The ^{11}B NMR resonances of the *B*H$_4$ moiety appeared at −35.9 (**4a**) and −33.5 (**4b**) ppm in benzene-d_6 with a difference of 2.4 ppm. However, for the present POCOP pincer palladium tetrahydroborate complexes, the ^{1}H NMR resonances of the B*H*$_4$ moiety appeared in relatively low field: 0.36 ppm for **3a** and 0.24 ppm for **3b** in benzene-d_6. The ^{11}B NMR resonances of the *B*H$_4$ moiety appeared at −39.82 ppm (**3a**) and −39.54 ppm (**3b**) in benzene-d_6 with a difference of only 0.28 ppm. The above NMR data indicate that the BH$_4$ moieties in the palladium complexes are less influenced by the pincer ligated metal center compared with the corresponding nickel complexes. This is consistent with the observations that **3a** and **3b** are unstable and can lose the BH$_3$ moiety easily to form the corresponding hydride species, while **4a** and **4b** are stable and the BH$_3$ moieties can only be partly removed by heating the complexes under a dynamic vacuum or completely removed by reacting the complexes with strong Lewis bases such as NEt$_3$ [28].

X-ray diffraction analyses were carried out to further characterize complexes **3a** and **3b**. The diffraction experiments were carried out at 296 K (for **3a**) and 100 K (for **3b**) using a SuperNova diffractometer (Oxford Diffraction). It should be noted that satisfactory crystallography data failed to be obtained for 3**b** at room temperature perhaps due to the thermal instability of this complex. The molecular structures of **3a** and **3b** are shown in Figs. 5 and 6 along with the selected bond lengths and angles.

As shown in Figs. 5 and 6, the geometries of the pincer backbones and the palladium centers of **3a** and **3b** are similar to those of **1a**, **1b**, **2a**, **2b** and other POCOP pincer palladium complexes [11,14]. Considering that relatively large errors exist in locating the

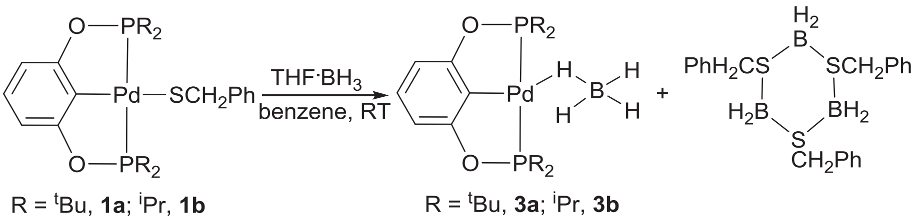

Scheme 3. Reactions of complexes **1a** and **1b** with BH$_3$·THF.

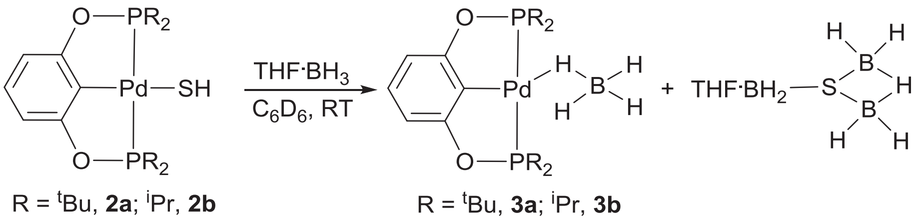

Scheme 4. Reactions of complexes **2a** and **2b** with BH_3·THF.

positions of the H atoms by X-ray diffraction, the B-H bond lengths and H-B-H bond angles agree with a tetrahedral geometry for the boron center. The Pd-H bond lengths (Pd1-Hb1a, 1.91(3) Å for **3a** and 1.78(3) Å for **3b**) are longer than those of the corresponding POCOP pincer palladium hydride complexes (1.53(4)–1.75(3) Å) [14]. The distances between the Pd atom and the other closely related H atom (Pd1···Hb1b, 2.11(3) Å for **3a** and 2.21(3) Å for **3b**) are significantly longer than the sum of the covalent radii of Pd and H (1.52 Å) [38]. The distances between the Pd atom and the B atom (Pd1···B1, 2.464(4) Å for **3a** and 2.420(3) Å for **3b**) are also much longer than the sum of the covalent radii of Pd and B (2.05 Å) [38]. This indicates that Hb1a is more closely coordinated to the Pd center compared with Hb1b.

For a transition metal tetrahydroborate complex, the coordination mode of the BH_4 ligand can be monodentate, bidentate or tridentate and the monodentate complex is the least stable [24,28,39–45]. The above crystallography data for complexes **3a** and **3b** favor a η^1-HBH_3 monodentate coordination mode for the BH_4 ligand in the solid state although the four hydrides are equivalent in solutions as suggested by the ^1H NMR spectra. It should be noted that the difference between Pd1-Hb1a (1.91(3) Å) and Pd1···Hb1b (2.11(3) Å) is only 0.20 Å in complex **3a**. Thus, the η^1-HBH_3 coordination mode should not be unambiguously established solely based on these crystallography data.

FTIR spectra were recorded using solid samples to further confirm the configuration of the Pd(BH_4) moiety in complexes **3a** and **3b**. The spectra (see Appendix A, Fig. A20–A21) also supported a monodentate coordination mode rather than other coordination modes [44,45]. For **3a**, the two ν(B-H_t) transitions appeared around 2390 cm^{-1} as a broad band; the single ν(B-H_b) band was shown at 2259 cm^{-1}; the weak ν(Pd-H_b) stretching vibration was displayed at 1571 cm^{-1}; the BH_3 deformation modes were exhibited at 994 and 1022 cm^{-1}. For **3b**, the two ν(B-H_t) transitions appeared at 2389 and 2370 cm^{-1}; the single ν(B-H_b) band was shown at 2212 cm^{-1}; the weak ν(Pd-H_b) stretching vibration was displayed at 1567 cm^{-1}; the BH_3 deformation modes were exhibited at 983 and 1029 cm^{-1}. The FTIR absorptions of the Pd(η^1-HBH_3) moiety in complexes **3a** and **3b** were also in agreement with those of other transition metal complexes bearing a η^1-HBH_3 monodentate BH_4 ligand [9,46–48].

3. Conclusions

In summary, we have synthesized and fully characterized several new POCOP pincer ligated palladium benzylthiolate and mercapto complexes, [2,6-$(R_2PO)_2C_6H_3$]$PdSCH_2Ph$ (R = ^{t}Bu, **1a**; ^{i}Pr, **1b**) and [2,6-$(R_2PO)_2C_6H_3$]PdSH (R = ^{t}Bu, **2a**; ^{i}Pr, **2b**). The reactions of these complexes with BH_3·THF produced exclusively the corresponding air/moisture sensitive thermally unstable tetrahydroborate complexes [2,6-$(R_2PO)_2C_6H_3$]Pd(η^1-HBH_3) (R = ^{t}Bu, **3a**; ^{i}Pr, **3b**) through Pd-S bond cleavage. X-ray crystallography and FTIR study supported a η^1-HBH_3 monodentate coordination mode for the BH_4 ligand in **3a** and **3b**. The boron induced C-S bond cleavage that was observed in the POCOP pincer ligated nickel benzylthiolate

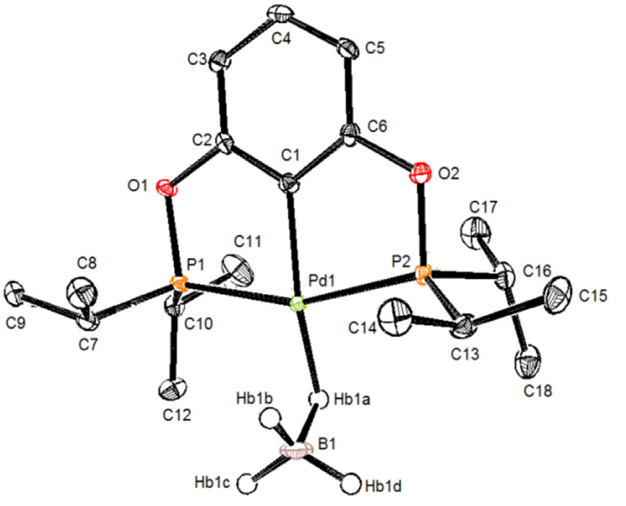

Fig. 5. Thermal ellipsoid plots of complex **3a** at the 50% probability level (hydrogen atoms except those attached to boron are omitted for clarity). Selected bond lengths (Å) and bond angles (deg): Pd1-C1, 2.006(2); Pd1-P1, 2.3039(6); Pd1-P2, 2.3049(6); Pd1-Hb1a, 1.91(3); Pd1···Hb1b, 2.11(3); Pd1···B1, 2.464(4); B1-Hb1a, 1.17(3); B1-Hb1b, 1.24(3); B1-Hb1c, 1.04(3); B1-Hb1d, 1.15(3); P1-Pd1-P2, 159.56(2); C1-Pd1-Hb1a, 154.2(9); P1-Pd1-Hb1a, 98.6(8); P2-Pd1-Hb1a, 99.3(8); Hb1a-B1-Hb1d, 111(2); Hb1a-B1-Hb1c, 111(2); Hb1a-B1-Hb1b, 108(2); Hb1d-B1-Hb1c, 113(2); Hb1d-B1-Hb1b, 105(2); Hb1c-B1-Hb1b, 108(2).

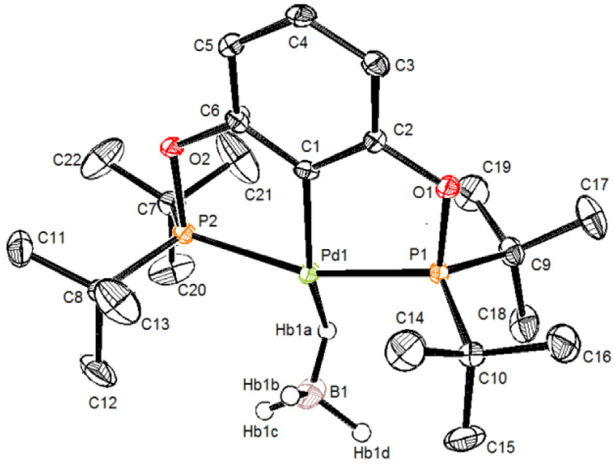

Fig. 6. Thermal ellipsoid plots of complex **3b** at the 50% probability level (hydrogen atoms except those attached to boron are omitted for clarity). Selected bond lengths (Å) and bond angles (deg): Pd1-C1, 1.9903(19); Pd1-P1, 2.2652(5); Pd1-P2, 2.2692(5); Pd1-Hb1a, 1.78(3); Pd1···Hb1b, 2.21(3); Pd1···B1, 2.420(3); B1-Hb1a, 1.28(2); B1-Hb1b, 1.15(2); B1-Hb1c, 1.10(3); B1-Hb1d, 1.06(3); P1-Pd1-P2, 159.39(2); C1-Pd1-Hb1a, 162.4(8); P1-Pd1-Hb1a, 99.0(8); P2-Pd1-Hb1a, 99.2(8); Hb1a-B1-Hb1c, 105.8(17); Hb1a-B1-Hb1d, 105.2(17); Hb1a-B1-Hb1b, 111.7(16); Hb1c-B1-Hb1d, 117.2(19); Hb1c-B1-Hb1b, 107.9(17); Hb1d-B1-Hb1b, 109.1(17).

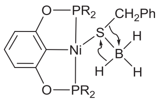

Chart 1. Interaction of the nickel benzylthiolate complex with BH$_3$.

complexes was not observed in the present palladium complexes perhaps due to the relatively weak Pd-S bond.

4. Experimental section

4.1. General information

The reactions and manipulations were carried out under a N$_2$ atmosphere. Solvents were degassed and dried using the standard procedures before use. Benzene-d_6 was distilled immediately from Na and benzophenone under a N$_2$ atmosphere before use. A Bruker Advance 400 MHz spectrometer was employed for recording the NMR spectra. Chemical shift values were calibrated internally to the residual solvent resonances for ^{1}H and ^{13}C NMR spectra and externally to 85% H$_3$PO$_4$ (δ 0) and BF$_3$·Et$_2$O (δ 0), respectively, for ^{31}P and ^{11}B NMR spectra. A Nicolet-Nexus 670 infrared spectrophotometer was used for recording the FTIR spectra. The palladium complexes [2,6-(^{t}Bu$_2$PO)$_2$C$_6$H$_3$]PdCl [49], [2,6-(^{i}Pr$_2$PO)$_2$C$_6$H$_3$]PdCl [14] and **1b** [11] were synthesized according to the published procedures.

4.2. Synthesis of [2,6-(^{t}Bu$_2$PO)$_2$C$_6$H$_3$]PdSCH$_2$Ph (*1a*)

To a suspension of NaH (240 mg, 10.0 mmol) in 20 mL of THF was added benzyl mercaptan dropwise (1.17 mL, 10.0 mmol) at 0 °C under a nitrogen atmosphere. The resulting mixture was warmed to room temperature and stirred for 1 h. A solution of [2,6-(^{t}Bu$_2$PO)$_2$C$_6$H$_3$]PdCl (1080 mg, 2 mmol) in THF (10 mL) was then added. The mixture was refluxed under a nitrogen atmosphere for 36 h. The volatiles were removed under vacuum and the residue was extracted with toluene and then filtered through a pad of Celite. Removal of toluene under vacuum produced complex **1a** as a yellow crystalline solid (978 mg, 78% yield). ^{1}H NMR (400 MHz, benzene-d_6, δ): 7.68 (d, 2H, ArH, $J_{\text{H-H}} = 7.1$ Hz), 7.23–7.27 (m, 2H, ArH), 7.07–7.10 (m, 1H, ArH), 6.92 (t, 1H, ArH, $J_{\text{H-H}} = 8.4$ Hz), 6.72 (d, 2H, ArH, $J_{\text{H-H}} = 8.4$ Hz), 4.11 (s, 1H, SCH_2Ph), 1.34–1.37 (m, 36H, C(CH_3)$_3$). ^{13}C{^{1}H} NMR (101 MHz, benzene-d_6, δ): 166.9 (t, ArC, $J_{\text{C-P}} = 5.6$ Hz), 146.8 (s, ArC), 136.2 (s, ArC), 129.1 (s, ArC), 128.2 (s, ArC), 127.9 (s, ArC), 125.9 (s, ArC), 105.6 (t, ArC, $J_{\text{C-P}} = 6.8$ Hz), 40.0 (t, C(CH$_3$)$_3$, $J_{\text{C-P}} = 7.8$ Hz), 38.5 (t, C(CH$_3$)$_3$, $J_{\text{C-P}} = 4.3$ Hz), 28.0 (t, C(CH$_3$)$_3$, $J_{\text{C-P}} = 3.8$ Hz). ^{31}P{^{1}H} NMR (162 MHz, benzene-d_6, δ): 194.4 (s). Anal. Calcd for C$_{29}$H$_{46}$PdO$_2$P$_2$S: C, 55.54; H, 7.39. Found: C, 55.33; H, 7.30.

4.3. Synthesis of [2,6-(^{t}Bu$_2$PO)$_2$C$_6$H$_3$]PdSH(*2a*)

A mixture of [2,6-(^{t}Bu$_2$PO)$_2$C$_6$H$_3$]PdCl (1080 mg, 2 mmol), NaSH (224 mg, 4 mmol) and THF (30 mL) was refluxed under a nitrogen atmosphere for 48 h. The volatiles were removed under vacuum and the residue was extracted with toluene and then filtered through a pad of Celite. Removal of toluene under vacuum produced complex **2a** as an orange crystalline solid (857 mg, 80% yield). ^{1}H NMR (400 MHz, benzene-d_6, δ): 6.90 (t, 1H, ArH, $J_{\text{H-H}} = 7.7$ Hz), 6.74 (d, 2H, ArH, $J_{\text{H-H}} = 7.7$ Hz), 1.30–1.33 (m, 36H, C(CH_3)$_3$), −0.74 (t, 1H, SH, $J_{\text{H-P}} = 10.3$ Hz). ^{13}C{^{1}H} NMR (101 MHz, benzene-d_6, δ): 166.8 (t, ArC, $J_{\text{C-P}} = 6.0$ Hz), 137.1 (t, ArC, $J_{\text{C-P}} = 9.8$ Hz), 127.9 (s, ArC), 105.7 (t, ArC, $J_{\text{C-P}} = 7.1$ Hz), 39.8 (t, C(CH$_3$)$_3$, $J_{\text{C-P}} = 8.2$ Hz), 27.8 (t, C(CH$_3$)$_3$, $J_{\text{C-P}} = 3.8$ Hz). ^{31}P{^{1}H} NMR (162 MHz, benzene-d_6, δ): 197.3 (s). Selected data from FTIR (KBr disc): 2960 (s), 2867 (s), 2587 (w), 1569 (m), 1439 (s), 841 (vs) cm^{-1}. Anal. Calcd for C$_{22}$H$_{40}$PdO$_2$P$_2$S: C, 49.21; H, 7.51. Found: C, 49.53; H, 7.74.

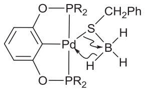

Chart 2. Interaction of the palladium benzylthiolate complex with BH$_3$.

4.4. Synthesis of [2,6-(^{i}Pr$_2$PO)$_2$C$_6$H$_3$]PdSH (*2b*)

Complex **2b** was prepared in 85% yield as a light yellow solid by a procedure similar to that used for **2a**. ^{1}H NMR (400 MHz, benzene-d_6, δ): 6.90 (t, 1H, ArH, $J_{\text{H-H}} = 7.8$ Hz), 6.74 (d, 2H, ArH, $J_{\text{H-H}} = 7.8$ Hz), 2.02–2.09 (m, 4H, CH(CH$_3$)$_2$), 1.18–1.24 (m, 12H, CH(CH_3)$_2$), 1.04–1.10 (m, 12H, CH(CH_3)$_2$), −1.03 (t, 1H, SH, $J_{\text{H-P}} = 11.9$ Hz). ^{13}C{^{1}H} NMR (101 MHz, benzene-d_6, δ): 166.1 (t, ArC, $J_{\text{C-P}} = 6.7$ Hz), 136.9 (t, ArC, $J_{\text{C-P}} = 3.5$ Hz), 128.1 (s, ArC), 106.6 (t, ArC, $J_{\text{C-P}} = 7.2$ Hz), 29.3 (t, CH(CH$_3$)$_2$, $J_{\text{C-P}} = 11.9$ Hz), 17.4 (t, CH(CH$_3$)$_2$, $J_{\text{C-P}} = 3.8$ Hz), 16.7 (s, CH(CH$_3$)$_2$). ^{31}P{^{1}H} NMR (162 MHz, benzene-d_6, δ): 192.1 (s). Selected data from FTIR (KBr disc): 2962 (s), 2927 (s), 2871 (m), 2567 (w), 1567 (m), 1441 (s), 839 (vs) cm^{-1}. Anal. Calcd for C$_{18}$H$_{32}$PdO$_2$P$_2$S: C, 44.96; H, 6.71. Found: C, 45.12; H, 6.86.

4.5. Reactions of *1a* and *1b* with BH$_3$·THF and characterization of *3a* and *3b*

Complex **1a** or **1b** (1 mmol) was dissolved in benzene (10 mL) in a flask under a nitrogen atmosphere; then BH$_3$·THF (2 mmol) was added. After the resulting mixture was stirred at room temperature for 1 h, the solution was concentrated to 5 mL and kept under a nitrogen atmosphere at room temperature for a few days. Colorless crystals of **3a** or **3b** precipitated. The crystals were separated from the mother solution, washed with pentane and stored under a nitrogen atmosphere at −30 °C.

For the reaction of **1a** with BH$_3$·THF, 350 mg (68% yield) of **3a** was isolated. ^{1}H NMR (400 MHz, benzene-d_6, δ): 6.86 (t, 1H, ArH, $J_{\text{H-H}} = 7.5$ Hz), 6.67 (d, 2H, ArH, $J_{\text{H-H}} = 7.5$ Hz), 1.30–1.33 (m, 36H, C(CH_3)$_3$), 0.36 (br q, 4H, BH_4, $J_{\text{H-B}} = 75$ Hz). ^{13}C{^{1}H} NMR (101 MHz, benzene-d_6, δ): 167.3 (t, ArC, $J_{\text{C-P}} = 5.3$ Hz), 133.4 (s, ArC), 128.4 (s, ArC), 105.9 (t, ArC, $J_{\text{C-P}} = 6.3$ Hz), 39.9 (t, C(CH$_3$)$_3$, $J_{\text{C-P}} = 7.9$ Hz), 27.6 (t, C(CH$_3$)$_3$, $J_{\text{C-P}} = 3.3$ Hz). ^{31}P{^{1}H} NMR (162 MHz, benzene-d_6, δ): 200.2 (s). ^{11}B NMR (128 MHz, benzene-d_6, δ): 39.8 (quin, $J_{\text{B-H}} = 82.4$ Hz). Selected data from FTIR (KBr disc): 3196 (vs), 2960 (m), 2390 (m), 2259 (m), 1571 (w), 1435 (vs), 1022 (s), 994 (s) cm^{-1}.

For the reaction of **1b** with BH$_3$·THF, 370 mg (80% yield) of **3b** was isolated. ^{1}H NMR (400 MHz, benzene-d_6, δ): 6.86 (t, 1H, ArH, $J_{\text{H-H}} = 7.5$ Hz), 6.68 (d, 2H, ArH, $J_{\text{H-H}} = 7.5$ Hz), 2.06–2.17 (m, 4H, CH(CH$_3$)$_2$), 1.18–1.24 (m, 12H, CH(CH_3)$_2$), 1.00–1.06 (m, 12H, CH(CH_3)$_2$), 0.24 (br q, 4H, BH_4, $J_{\text{H-B}} = 77$ Hz). ^{13}C{^{1}H} NMR (101 MHz, benzene-d_6, δ): 166.5 (t, ArC, $J_{\text{C-P}} = 6.6$ Hz), 133.8 (t, ArC, $J_{\text{C-P}} = 2.8$ Hz), 128.5 (s, ArC), 106.2 (t, ArC, $J_{\text{C-P}} = 7.3$ Hz), 29.0 (t, CH(CH$_3$)$_2$, $J_{\text{C-P}} = 12.2$ Hz), 17.0 (t, CH(CH$_3$)$_2$, $J_{\text{C-P}} = 3.9$ Hz), 16.5 (s, CH(CH$_3$)$_2$). ^{31}P{^{1}H} NMR (162 MHz, benzene-d_6, δ): 195.4 (s). ^{11}B NMR (128 MHz, benzene-d_6, δ): 39.5 (quin, $J_{\text{B-H}} = 81.0$ Hz). Selected data from FTIR (KBr disc): 2962 (s), 2928 (s), 2871 (m), 2389 (m), 2370 (m), 2212 (m), 1567 (w), 1440 (vs), 1029 (s), 983 (s) cm^{-1}.

4.6. Reactions of *2a* and *2b* with BH$_3$·THF

The reactions of complex **2a** and **2b** with BH$_3$·THF were carried out in NMR tubes. Under a nitrogen atmosphere, **2a** or **2b** (0.1 mmol) was mixed with 6 equiv of BH$_3$·THF in a NMR tube containing 0.5 mL of benzene-d_6. The reaction was monitored by

Table 1
Summary of crystal data and structure refinement for complexes **1a**, **1b**, **2a**, **2b**, **3a** and **3b**.

	1a	1b	2a	2b	3a	3b
Empirical formula	$C_{29}H_{46}O_2P_2PdS$	$C_{25}H_{38}O_2P_2PdS$	$C_{22}H_{40}O_2P_2PdS$	$C_{18}H_{32}O_2P_2PdS$	$C_{22}H_{43}BO_2P_2Pd$	$C_{18}H_{35}BO_2P_2Pd$
Formula weight	627.06	570.95	536.94	480.83	518.71	462.61
Temp, K	288.99(10)	297.00(10)	293.94(10)	294.27(10)	296.15	99.99(10)
Crystal system	Monoclinic	Monoclinic	Triclinic	Triclinic	Triclinic	Triclinic
Space group	P 21/c	P 1 21/c 1	P −1	P −1	P −1	P −1
a, Å	20.1387(4)	15.9773(8)	8.3164(6)	8.1509(3)	8.2831(7)	7.76124(14)
b, Å	10.66230(10)	15.3737(8)	12.2615(10)	10.3927(3)	12.2518(10)	11.8938(3)
c, Å	15.6302(3)	22.9689(8)	13.4694(11)	14.5842(5)	13.4218(11)	12.0861(3)
α (°)	90	90	100.348(7)	100.373(3)	100.8650(10)	96.4669(18)
β (°)	112.738(2)	97.524(4)	95.609(7)	104.468(3)	95.5030(10)	94.4646(16)
γ (°)	90	90	105.021(7)	102.456(3)	104.3080(10)	94.7522(17)
Volume, Å^3	3095.36(10)	5593.3(4)	1289.86(19)	1131.76(7)	1281.56(18)	1100.48(4)
Z	4	8	2	2	2	2
d_{calc}, g cm^{-3}	1.346	1.356	1.382	1.411	1.344	1.396
λ, Å	1.54184	0.71073	0.71073	1.54184	0.71073	0.71073
μ, mm^{-1}	6.613	0.871	0.939	8.867	0.863	0.996
No. of data collected	13838	37115	9865	12704	9026	12562
No. of unique data	5589	10377	4586	4380	4547	3926
R_{int}	0.0205	0.0449	0.0627	0.0448	0.0163	0.0253
Goodness-of-fit on F^2	1.068	1.107	0.954	1.048	1.061	1.053
R_1, wR_2 ($I > 2\sigma(I)$)	0.0302, 0.0801	0.0771, 0.1692	0.0515, 0.0912	0.0318, 0.0806	0.0251, 0.0579	0.0200, 0.0451
R_1, wR_2 (all data)	0.0325, 0.0817	0.1012, 0.1813	0.0858, 0.1012	0.0349, 0.0843	0.0275, 0.0593	0.0214, 0.0456

^{31}P{^{1}H} and ^{11}B NMR spectra at room temperature. Both the reactions were completed in 30 min; the NMR spectra showed the formation **3a** or **3b** and THF·BH_2-μ_2-S(B_2H_5).

4.7. *X-ray structure determination*

Single crystals of complexes **1a**, **1b**, **2a** and **2b** used for X-ray diffraction analyses were obtained from *n*-hexane/toluene solutions at room temperature. Single crystals of complexes **3a** and **3b** used the diffraction experiments were obtained from the concentrated benzene reaction solutions at room temperature. Intensity data were collected on a SuperNova diffractometer (Oxford Diffraction) at room temperature (for **1a**, **1b**, **2a**, **2b** and **3a**) or 100 K (for **3b**). Mirror-monochromated Cu Kα radiation ($\lambda = 1.54184$ Å) was used for **1b** and **2a**; mirror-monochromated Mo Kα radiation ($\lambda = 0.71073$ Å) was used for **1a**, **2b** and **3b**; graphite-monochromated Mo Kα radiation ($\lambda = 0.71073$ Å) was used for **3a**. Data processing and structure refinement were performed as described in our previous publication [21]. Two independent molecules were found in the crystalline lattice of complex **1b**. No solvent of was crystallized in the lattice for any of the structures. The crystallographic data and structure refinement for these POCOP pincer palladium complexes is summarized in Table 1.

CCDC 1872773 (**1a**), 1872774 (**1b**), 1872771 (**2a**), 1872772 (**2b**), 1872775 (**3a**) and 1872776 (**3b**) contain the supplementary crystallographic data for this paper. These data can be obtained free of charge from The Cambridge Crystallographic Data Center.

Conflicts of interest

The authors declare no conflict of interest.

Acknowledgements

This work was supported by the National Natural Science Foundation of China (Grant Numbers 21571052 and 21771057).

Appendix A. Supplementary data

Supplementary data to this article can be found online at https://doi.org/10.1016/j.jorganchem.2018.12.019.

References

[1] F. Pan, Z.-J. Shi, ACS Catal. 4 (2014) 280–288.
[2] H. Prokopcová, C.O. Kappe, Angew. Chem. Int. Ed. 48 (2009) 2276–2286.
[3] S.R. Dubbaka, P. Vogel, Angew. Chem. Int. Ed. 44 (2005) 7674–7684.
[4] S.G. Modha, V.P. Mehta, E.V. van der Eycken, Chem. Soc. Rev. 42 (2013) 5042–5055.
[5] T. Shibata, A. Mitake, Y. Akiyamac, K.S. Kanyiva, Chem. Commun. 53 (2017) 9016–9019.
[6] J. Li, Y. An, J. Li, S. Yang, W. Wu, H. Jiang, Org. Chem. Front. 4 (2017) 1590–1594.
[7] Y. Huang, X. Li, X. Wang, Y. Yu, J. Zheng, W. Wu, H. Jiang, Chem. Sci. 8 (2017) 7047–7051.
[8] J. Zhang, T. Liu, Q.-Q. Ma, S. Li, X. Chen, Dalton Trans. 47 (2018) 6018–6024.
[9] E. Alberico, P. Sponholz, C. Cordes, M. Nielsen, H.-J. Drexler, W. Baumann, H. Junge, M. Beller, Angew. Chem. Int. Ed. 52 (2013) 14162–14166.
[10] A.A. Koridze, S.A. Kuklin, A.M. Sheloumov, F.M. Dolgushin, V. Yu Lagunova, I.I. Petukhova, M.G. Ezernitskaya, A.S. Peregudov, P.V. Petrovskii, E.V. Vorontsov, M. Baya, R. Poli, Organometallics 23 (2004) 4585–4593.
[11] Q.-Q. Ma, T. Liu, S. Li, J. Zhang, X. Chen, H. Guan, Chem. Commun. 52 (2016) 14262–14265.
[12] J. Zhang, C.M. Medley, J.A. Krause, H. Guan, Organometallics 29 (2010) 6393–6401.
[13] K. Osakada, Y. Ozawa, A. Yamamoto, J. Chem. Soc., Dalton Trans. (1991) 759–764.
[14] A. Adhikary, J.R. Schwartz, L.M. Meadows, J.A. Krause, H. Guan, Inorg. Chem. Front. 1 (2014) 71–82.
[15] B. Vabre, M.D. Spasyuk, D. Zargarian, Organometallics 31 (2012) 8561–8570.
[16] B. Vabre, P. Petiot, R. Declercq, D. Zargarian, Organometallics 33 (2014) 5173–5184.
[17] J. Hao, B. Vabre, D. Zargarian, Organometallics 33 (2014), 6568-5676.
[18] S. Lapointe, B. Vabre, D. Zargarian, Organometallics 34 (2015) 3520–3531.
[19] J. Zhang, A. Adhikary, K.M. King, J.A. Krause, H. Guan, Dalton Trans. 41 (2012) 7959–7968.
[20] T. Liu, W. Meng, Q.-Q. Ma, J. Zhang, H. Li, S. Li, Q. Zhao, X. Chen, Dalton Trans. 46 (2017) 4504–4509.
[21] J. Zhang, T. Liu, C. Wei, J. Chang, Q.-Q. Ma, S. Li, N. Ma, X. Chen, Chem. Asian J. 13 (2018) 3231–3238.
[22] J. Zhang, J. Chang, T. Liu, B. Cao, Y. Ding, X. Chen, Catalysts 8 (2018) 508.
[23] T.J. Schmeier, A. Nova, N. Hazari, F. Maseras, Chem. Eur J. 18 (2012) 6915–6927.
[24] A. Rossin, M. Peruzzini, F. Zanobini, Dalton Trans. 40 (2011) 4447–4452.
[25] T.J. Schmeier, N. Hazari, C.D. Incarvito, J.A. Raskatov, Chem. Commun. 47 (2011) 1824–1826.
[26] B.J. Boro, E.N. Duesler, K.I. Goldberg, R.A. Kemp, Inorg. Chem. 48 (2009) 5081–5087.
[27] S. Chakraborty, J. Zhang, J.A. Krause, H. Guan, J. Am. Chem. Soc. 132 (2010) 8872–8873.
[28] S. Chakraborty, J. Zhang, Y.J. Patel, J.A. Krause, H. Guan, Inorg. Chem. 52 (2013) 37–47.
[29] H. Li, W. Meng, A. Adhikary, S. Li, N. Ma, Q. Zhao, Q. Yang, N.A. Eberhardt, K.M. Leahy, J.A. Krause, J. Zhang, X. Chen, H. Guan, J. Organomet. Chem. 804 (2016) 132–141.
[30] Q.-Q. Ma, T. Liu, A. Adhikary, J. Zhang, J.A. Krause, H. Guan, Organometallics 35 (2016) 4077–4082.

[31] K. Osakada, Y. Ozawa, A. Yamamoto, Bull. Chem. Soc. Jpn. 64 (1991) 2002–2004.
[32] M. Basauri-Molina, S. Hernández-Ortega, R.A. Toscano, J. Valdés-Martínez, D. Morales-Morales, Inorg. Chim. Acta. 363 (2010) 1222–1229.
[33] Y.-J. Kim, K.-Y. Choi, S.G. Lee, Z.N. Zheng, S.W. Lee, Bull. Korean Chem. Soc. 35 (2014) 1205–1208.
[34] M.L. Buil, S. Elipe, M.A. Esteruelas, E. Oñate, E. Peinado, N. Ruiz, Organometallics 16 (1997) 5748–5755.
[35] D.A. Vicic, W.D. Jones, J. Am. Chem. Soc. 119 (1997) 10855–10856.
[36] M. Di Vaira, M. Peruzzini, P. Stoppioni, Inorg. Chem. 30 (1991) 1001–1007.
[37] H. Binder, A. Ziegler, R. Ahlrichs, H. Schiffer, Chem. Ber. 120 (1987) 1545–1552.
[38] P. Pyykkö, M. Atsumi, Chem. Eur J. 15 (2009) 186–197.
[39] E.J. Corey, N.J. Cooper, W.M. Canning, W.N. Lipscomb, T.F. Koetzle, Inorg. Chem. 21 (1982) 192–199.
[40] A.J. Churchard, M.K. Cyranski, Ł. Dobrzycki, A. Budzianowski, W. Grochala, Energy Environ. Sci. 3 (2010) 1973–1978.
[41] Y. Journaux, V. Lozan, J. Klingele, B. Kersting, Chem. Commun. (2006) 83–84.
[42] M. Kandiah, G.S. McGrady, A. Decken, P. Sirsch, Inorg. Chem. 44 (2005) 8650–8652.
[43] P.J. Desrochers, S. LeLievre, R.J. Johnson, B.T. Lamb, A.L. Phelps, A.W. Cordes, W. Gu, S.P. Cramer, Inorg. Chem. 42 (2003) 7945–7950.
[44] T.J. Marks, J.R. Kolb, Chem. Rev. 77 (1977) 263–293.
[45] T.J. Marks, W.J. Kennelly, J.R. Kolb, L.A. Shimp, Inorg. Chem. 11 (1972) 2540–2546.
[46] C. Bornschein, S. Werkmeister, B. Wendt, H. Jiao, E. Alberico, W. Baumann, H. Junge, K. Junge, M. Beller, Nat. Commun. 5 (2014) 4111.
[47] I. Koehne, T.J. Schmeier, E.A. Bielinski, C.J. Pan, P.O. Lagaditis, W.H. Bernskoetter, M.K. Takase, C. Würtele, N. Hazari, S. Schneider, Inorg. Chem. 53 (2014) 2133–2143.
[48] M.V. Baker, L.D. Field, Appl. Organomet. Chem. 4 (1990) 543–549.
[49] A.V. Polukeev, S.A. Kuklin, P.V. Petrovskii, S.M. Peregudova, A.F. Smol'yakov, F.M. Dolgushin, A.A. Koridze, Dalton Trans. 40 (2011) 7201–7209.